# Using a UWB Radar Imaging Method with Five Antennas on a Target with Arbitrary Translation and Rotation Motion

Takuya Sakamoto*, Toru Sato*
*Graduate School of Informatics, Kyoto University
Yoshida-Honmachi, Sakyo-ku, 606-8501 Kyoto, Japan, t-sakamo@i.kyoto-u.ac.jp

***Abstract*—Developing usable technologies for indoor target detection is currently a topic of great interest. Ultra wide-band (UWB) radar is promising in this regard because of its high range-resolution. However, conventional UWB radar imaging systems are costly and impractical since they require a large antenna array to obtain high spatial resolution. This study proposes a new imaging method for a simple UWB radar system using the motion of the target. The imaging method employs five antennas for estimating the motion of a target, including its rotation. Previous work deals only with the translation motion of a target ignoring the rotation, which makes the method impractical. The proposed method, an extension of the previous method, obtains an accurate image for an unknown-shaped target with arbitrary translation and rotation. Numerical simulation results show that the proposed method is able to estimate the target's shape and its motion.**

## I. Introduction

Security surveillance systems are in demand because of increased criminal threats. Ultra wideband (UWB) radar is a promising technology for this purpose, because of its advantages such as accurate distance measurement, which are not found in conventional camera-based systems. Although a number of imaging methods have been proposed, most of these methods require large antenna arrays. For radar imaging, Jofre et al. [1] showed that the number of antennas has a significant effect on image quality. This means that there is a lower bound on the number of antennas needed to obtain the required resolution with conventional methods. In fact, Leuschen and Plumb [2] and Yarovoy et al. [3] employed 50 and 13 antennas, respectively, to obtain acceptable image quality in ground-penetrating radar imaging. To realize a simple and cost-effective UWB radar system, a new technology needs to be developed. Huang et al. [4] introduced compressive sensing to reduce the number of antennas. They reduced the total number of antennas from 51 to 10 while maintaining the same sidelobe level in the image.

Another UWB radar imaging method with a reduced number of antennas was proposed by Matsuki et al. [5]. This method makes use of the motion of the target to reduce the array elements and is similar to the Inverse Synthetic Aperture Radar (ISAR) techniques [6], [7], since both employ the motion of the target to improve image quality. However, for our intended application, the problem is more complex, because the target is relatively close to the antennas. This shifts the scattering centers on the target surface, depending on the relative positions of the antenna and target. In addition, the target motion cannot be modeled as a simple function because it is basically arbitrary. The method in [5] has been shown to be effective, because the system can be simplified and produced at a lower cost than conventional large array-based systems. The method assumes that a target moves in an unknown orbit, but without rotating. However, this assumption is not always relevant, because a target can change its viewing angle depending on its direction of movement. Since this paper aims to develop an imaging method for a target in the near field, the motion of the scattering center must be considered. This study presents a UWB radar system with five antennas for simultaneous estimation of a target's shape, translation and rotation. The performance of the proposed method is established through numerical simulations.

## II. System Model

Assuming a 2-dimensional model for simplicity, we aim to estimate a 2-dimensional target shape. A 5-element linear antenna array is installed at fixed intervals of $\Delta x = 0.2\mathrm{m}$ on a straight line as depicted in Fig. 1. The straight line could correspond to a wall or the ceiling in a hallway, with the problem defined as the imaging of the cross section of a human body walking down the hallway.

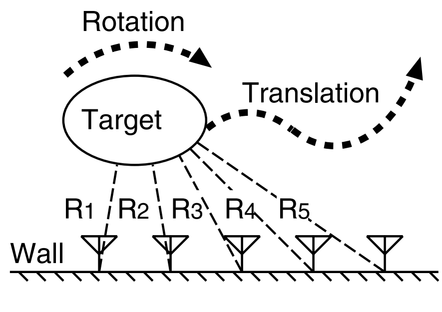


Fig. 1. Assumed system model.

Each of the antennas is connected to a UWB pulse generator and a receiver. In addition, each antenna is operated as a monostatic radar system with modulation that avoids interference among the antennas. Any modulation values can be used here as long as they are orthogonal to one another to realize a kind of multiple access system. Pulses are simultaneously transmitted from each antenna at time intervals of $\Delta t$, and echoes are received at the same antenna. The imaging methods proposed in this paper employs only the delay time of echoes, which must be measured accurately. The transmitted ultra-wideband waveforms should satisfy this condition.

The target is assumed to have an unknown boundary $(X_0(\xi), Y_0(\xi))$, where $0 \le \xi \le 2\pi$ is a parameter. The centroid of the target is at the origin of the assumed coordinates. Under this condition, we can define rotation around the origin independently of the shape of the target. The target moves with a translation motion $(X_{\rm T}(t), Y_{\rm T}(t))$ and a rotation $\phi(t)$ at time $t$. The target boundary $(X(\xi,t), Y(\xi,t))$ at time $t$ is expressed as

$$\begin{bmatrix} X(\xi,t) \\ Y(\xi,t) \end{bmatrix} = R(\phi(t)) \begin{bmatrix} X_0(\xi) \\ Y_0(\xi) \end{bmatrix} + \begin{bmatrix} X_{\rm T}(t) \\ Y_{\rm T}(t) \end{bmatrix}, \quad (1)$$

where $R(\phi)$ denotes the rotation matrix

$$R(\theta) = \begin{pmatrix} \cos\theta & -\sin\theta \\ \sin\theta & \cos\theta \end{pmatrix}. \quad (2)$$

The distance between each antenna and the scattering center of the target is measured as $R_i(t)$ $(i = 1, 2, \cdots, 5)$ using the $i$-th antenna at each time step $t_n = n\Delta t$. The purpose of this paper is to develop a method to estimate the translation $(X_{\rm T}(t), Y_{\rm T}(t))$, rotation $\phi(t)$, and shape $(X_0(\xi), Y_0(\xi))$ of a target using the range data $R_i(t)$ $(i = 1, 2, \cdots, 5)$.

## III. Proposed Method

Matsuki [5] proposed a method for estimating a target's translation motion and shape, based on a fitting method using a circle. Because a circle has three degrees of freedom, three antennas are used. However, this method cannot estimate the target's rotation because of the symmetry of a circle. We propose a new method using an ellipse rather than a circle to estimate both the rotation and translation to obtain a target image.

### A. Motion Estimation by Optimization with an Elliptical Shape Model

The proposed method estimates a local target shape at each time step $t = t_n$ using an elliptical model with five parameters $a, b, x_0, y_0$, and $\theta$. The ellipse is expressed as

$$\begin{aligned} & \left(\frac{\cos^2\theta}{a^2} + \frac{\sin^2\theta}{b^2}\right)(x - x_0)^2 \\ + & \left(\frac{\sin^2\theta}{a^2} + \frac{\cos^2\theta}{b^2}\right)(y - y_0)^2 \\ + & \sin 2\theta \left(\frac{1}{a^2} - \frac{1}{b^2}\right)(x - x_0)(y - y_0) = 1, \end{aligned} \quad (3)$$

where $a$ and $b$ are the long and short axes of the ellipse, $(x_0, y_0)$ is the center of the ellipse, and $\theta$ is the rotational angle. The distance between the $i$-th antenna and the corresponding scattering center $\boldsymbol{c}_i(a, b, x_0, y_0, \theta)$ is defined as $r_i(a, b, x_0, y_0, \theta)$. These variables $\boldsymbol{c}_i$ and $r_i$ are calculated using the $i$-th antenna position $\boldsymbol{x}_i$. The scattering center $\boldsymbol{c}_i(a, b, x_0, y_0, \theta)$ is equivalent to the point on the ellipse that is closest to antenna $\boldsymbol{x}_i$ because there is no point closer to the antenna than the foot of a perpendicular on such a convex curve.

We define a cost function

$$\begin{aligned} & F_n(a, b, x_0, y_0, \theta) \\ = & \sum_{i=1}^{N_{\rm a}} |r_i(a, b, x_0, y_0, \theta) - R_i(t_n)|^2, \end{aligned} \quad (4)$$

where $N_{\rm a} = 5$ is the number of antennas. By minimizing this cost function, we determine the most likely parameter set of an ellipse as

$$(a_n, b_n, x_{0n}, y_{0n}, \theta_n) = \arg\min F_n(a, b, x_0, y_0, \theta). \quad (5)$$

To perform this optimization process, we need to calculate the scattering center points $\boldsymbol{c}_{n,i}$ $i = 1, 2, \cdots, 5$ at each time step $t = t_n$. To calculate these scattering centers, we use the optimized parameters of ellipse $(x_{0n}, y_{0n}, a_n, b_n, \theta_n)$ and each antenna's position $\boldsymbol{x}_i$. The scattering center point $\boldsymbol{c}_{n,i}$ is estimated as the foot of the perpendicular drawn through the $i$-th antenna position. This process can be computed analytically, as detailed in the appendix. The Levenberg-Marquardt algorithm is used to optimize Eq. (5) using the analytical expression of the scattering centers. This Levenberg-Marquardt algorithm is known to be fast and stable for minimization problems if the optimum cost function value is close to zero [8].

### B. Phase Ambiguity in Estimating Rotational Motion

The parameters $(x_0, y_0)$ and $\theta$ correspond to the translation and rotation of the target. Note that $\theta$ is ambiguous with an integer-multiple of $\pi$; all models expressed with $\theta + m\pi$ are identical, where $m$ is an arbitrary integer. Because of this ambiguity, the estimated rotational motion can have discontinuities, making it difficult to estimate the rotation accurately. Consequently, we select the rotational angle that is closest to the previously estimated angle as

$$m = \arg\min |\theta_n - \theta_{n-1} + m\pi|^2, \quad (6)$$

where $\theta_n$ is the estimated rotational angle at time $t_n$, minimizing the gap between two adjacent angles. Then, $\theta_n$ is updated as $\theta_n \leftarrow \theta_n + m\pi$ to estimate the rotation.

### C. Imaging Process Compensating for Target Motion

The target shape is obtained from the target motion estimated using the procedure described in the previous sections. The image is estimated from the scattering centers by compensating for the motion. The scattering centers are used because the elliptical model locally approximates the target shape around the scattering centers and it is not relevant to use the entire elliptical shape estimated from the optimization process. Note that the scattering centers have already been calculated in Eq. (5) because $r_i(a, b, x_0, y_0, \theta)$ corresponds to the distance between scattering center $\boldsymbol{c}_{n,i}$ and antenna position $\boldsymbol{x}_i$. The next step is to compensate for $(x_0, y_0)$ and $\theta$ to estimate the target shape in the initial state $t = 0$ as

$$\left[\begin{array}{c} \hat{X}_0^{(n,i)} \\ \hat{Y}_0^{(n,i)} \end{array}\right] = R(-\theta_n)\left(\boldsymbol{c}_{n,i} - \left[\begin{array}{c} x_{0n} \\ y_{0n} \end{array}\right]\right). \quad (7)$$

## IV. Performance Evaluation through Numerical Simulation

### A. Application to an Elliptical Target

The performance of the proposed method is evaluated through numerical simulation. Fig. 2 shows an elliptical target moving to the right and rotating clockwise. We set the actual shape parameters as $a = 0.15$ m, $b = 0.10$ m, $\theta = -\pi/4$ rad, the translation as

$$X_{\mathrm{T}} = X_0 + v_x t, \quad (8)$$

$$Y_{\mathrm{T}} = Y_{\mathrm{T0}} + Y_{\mathrm{Ts}} \sin(\omega_0 t + \chi_0), \quad (9)$$

and the rotation as

$$\phi(t) = \phi_0 \sin(\omega_\phi t), \quad (10)$$

where $X_0 = -0.4$ m, $v_x = 2.0$ m/sec, $Y_{\mathrm{T0}} = 0.5$ m, $Y_{\mathrm{Ts}} = 0.1$ m, $\omega_0 = 2\pi$ rad/sec, $\chi_0 = \pi/3$ rad, $\phi_0 = 1.3\pi$ rad, and $\omega_\phi = \pi$ rad/sec. The sampling interval is set as $\Delta t = 5.0$ msec.

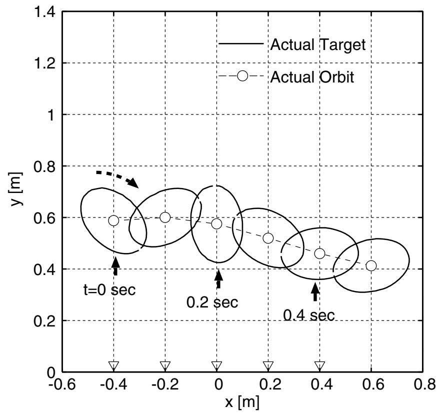


Fig. 2. Assumed elliptical target shape and motion with rotation.

The five triangles on the $x$-axis in Fig. 2 show the antenna positions. Here, we explain the results obtained by applying the proposed method. The solid lines and white circles in this figure show snapshots of the target and the actual center positions of the target. The black dots in Fig. 3 show the estimated scattering centers $\boldsymbol{c}_{n,i}$, which are accurately located on the actual target boundaries (solid lines). These scattering centers are calculated using the parameters optimized in Eq. (5) at each time step. Five scattering centers are estimated for each snapshot, because there are five antennas. These points are transformed to the initial positions at $t = 0$ by compensating for the motion as in Eq. (7) to finally obtain the target image in Fig. 4. The target shape is accurately estimated using the proposed method, since the actual target shape is elliptical, identical to the assumed elliptical model.

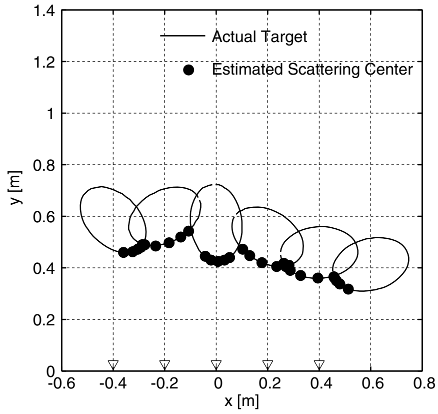


Fig. 3. Estimated scattered points for an elliptical target.

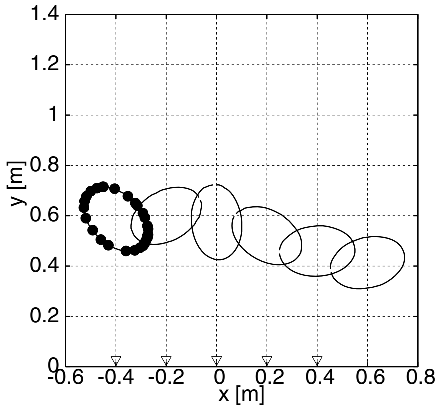


Fig. 4. Estimated elliptical target shape after compensation for the motion.

### B. Application to a Slightly Distorted Non-Elliptical Target

In this section, we investigate the performance of the proposed method for a non-elliptical target. We assume a target shape expressed as follows:

$$\left[\begin{array}{c} X_0(\xi) \\ Y_0(\xi) \end{array}\right] = \left[\begin{array}{c} a(1 + \delta\cos\xi)\cos\xi \\ b(1 + \delta\cos(\xi + \pi/4))\sin\xi \end{array}\right]. \quad (11)$$

Some examples of this target shape model are depicted in Fig. 5. The target shape is distorted as $\delta$ increases from 0.0 to 0.3, where $\delta = 0.0$ corresponds to the elliptical model considered in the previous section.

The measured distances to the target from the five antennas are shown in Fig. 6. Here, the assumed target motion is the same as in the previous section. Although the target shape is relatively simple, the measured distances show complicated curves because of the target motion.

Next, we present the results of the proposed method applied to the non-elliptical target with $\delta = 0.1$. The dashed lines in Fig. 7 show the elliptical models optimized using the proposed method. The estimated elliptical models are not identical to the actual target shape, changing its size. This is because the algorithm estimates the elliptical model using the local shape of the target, not the whole shape. Consequently, the actual and

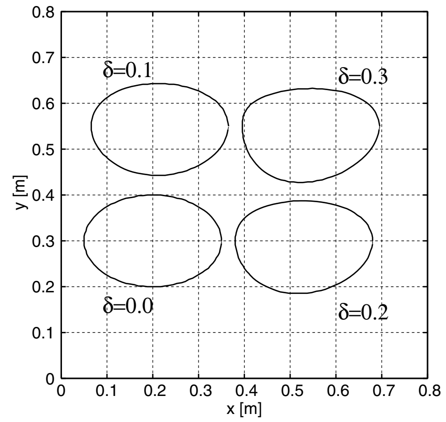


Fig. 5. Assumed non-elliptical target shapes with different $\delta$ values.

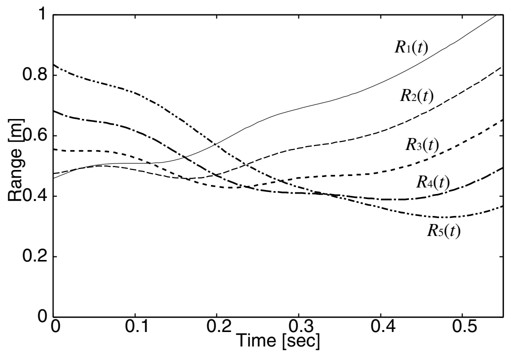


Fig. 6. Measured range data using 5 antennas for a non-elliptical target $\delta = 0.1$.

estimated curves match only around the scattering centers. The estimated $(x_0, y_0)$ center position of the estimated elliptical model, corresponding to the estimated translation motion, is shown as the dashed line in Fig. 8. The estimation accuracy is not high enough in certain parts, $x = -0.2$ m and $x = 0.1$ m in this figure. Fig. 9 shows the actual and estimated rotation angles. Although the estimation is accurate at the beginning and the end, we see that the rotational angle estimation is poor when the translation estimation is also inaccurate, giving a maximum estimation error of 25.8 degrees.

Fig. 10 depicts images of the actual and estimated shapes for $\delta = 0.1$ The whole shape is roughly estimated, but the accuracy is lower than that for the elliptical target. This is because an elliptical model is used for local fitting, but with a target shape that is not elliptical. The difference between the model and the actual target results in lower accuracy. The root-mean-square (RMS) error is 23.34 mm for the estimation. Note that the RMS error $\varepsilon$ is calculated as

$$\varepsilon = \sqrt{\frac{1}{N_\mathrm{a} N_\mathrm{obs}} \sum_{n=1}^{N_\mathrm{obs}} \sum_{i=1}^{N\mathrm{a}} \left( \hat{\boldsymbol{X}}_{n,i} - \boldsymbol{p}_{n,i} \right)^2}, \qquad (12)$$

where $\hat{\boldsymbol{X}}_{n,i} = (\hat{X}_0^{(n,i)}, \hat{Y}_0^{(n,i)})$ is the point estimated using the $i$-th antenna at the $n$-th time-step, and $\boldsymbol{p}_{n,i}$ is the point on the actual target surface that is closest to the estimated point $\hat{\boldsymbol{X}}_{n,i}$.

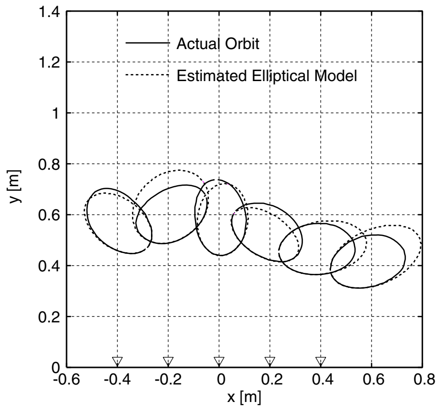


Fig. 7. Estimated elliptical models for non-elliptical target ($\delta = 0.1$).

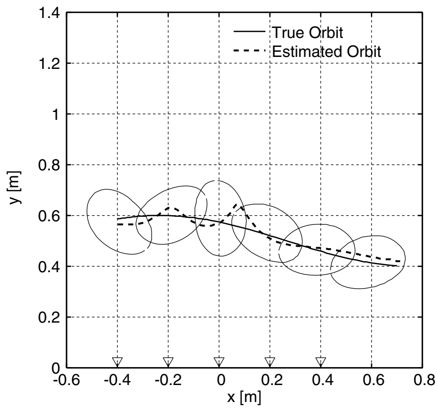


Fig. 8. Actual and estimated translation orbits using the proposed method for a non-elliptical target ($\delta = 0.1$).

## V. Conclusion

We have proposed new imaging methods for UWB radar using five antennas. The methods use the motion of the target, including translation and rotation. The local shape of a target is approximated with an ellipse, and the parameters of the elliptic model are used to estimate the target motion. The method is capable of estimating a target shape by compensating for the estimated motion. The proposed method works well for an elliptical target, and with some degree of accuracy for a slightly distorted non-elliptical target. An important future task is to expand the method so that it can be applied to more distorted target shapes.

## References

[1] L. Jofre, A. Broquetas, J. Romeu, S. Blanch, A. P. Toda, X. Fabregas, and A. Cardama, "UWB tomographic radar imaging of penetrable and impenetrable objects" Proceedings of the IEEE, vol. 97, no. 2, pp. 451–464, 2009.

[2] C. J. Leuschen and R. G. Plumb, "A matched-filter-based reverse-time migration algorithm for ground-penetrating radar data," IEEE Trans. Geoscience & Remote Sensing, vol. 39, no. 5, pp. 929–936, May 2001.

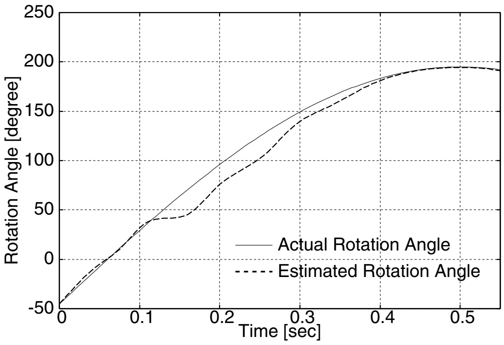


Fig. 9. Actual and estimated rotation angle using the proposed method ($\delta = 0.1$).

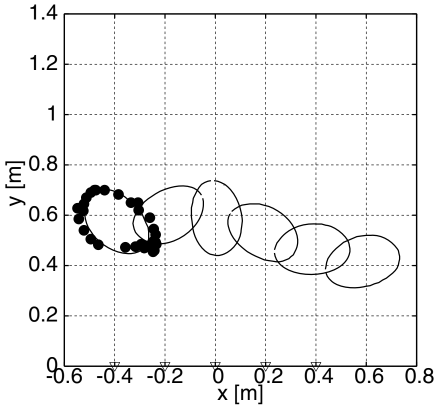


Fig. 10. Actual and estimated target shapes for a non-elliptical target using the proposed method ($\delta = 0.1$).


[3] A. G. Yarovoy, T. G. Savelyev, P. J. Aubry, P. E. Lys, and L. P. Ligthart, "UWB array-based sensor for near-field imaging," IEEE Transactions on Microwave Theory and Techniques, vol. 55, no. 6, part 2, pp. 1288-1295, June 2007.

[4] Q. Huang, L. Qu, B. Wu, and G. Fang, "UWB through-wall imaging based on compressive sensing," IEEE Transactions on Geoscience and Remote Sensing, vol. 48, no. 3, pp. 1408–1415, March 2010.

[5] Y. Matsuki, T. Sakamoto and T. Sato, "Study of a method for 2-D imaging of simple-shaped targets with arbitrary motion using UWB radar with a small number of antennas," Proc. 20th International Conference on Applied Electromagnetics and Communications, Sep. 2010.

[6] G. Y. Lu and Z. Bao, "Compensation of scatterer migration through resolution cell in inverse synthetic aperture radar imaging," IEE Proceedings Radar, Sonar and Navigation, vol. 147, no. 2, pp. 80–85, Apr. 2000.

[7] Z. Li, S. Papson, and R. M. Narayanan, "Data-level function of multilook inverse synthetic aperture radar images," IEEE Transactions on Geoscience and Remote Sensing, vol. 46, no. 5, May 2008.

[8] D. Marquardt, "An algorithm for least-squares Estimation of Nonlinear Parameters," SIAM Journal on Applied Mathematics, vol. 11, pp. 431–441, 1963.